Electronic Supporting Information for

Core-shell structured PtRu nanoparticles@FeP promoter with efficient nanointerface for alcohol fuels electrooxidation

Yufei Bao, Fulong Wang, Xiaocong Gu and Ligang Feng*

School of Chemistry and Chemical Engineering, Yangzhou University, Yangzhou, 225002, China.

*Corresponding authors.

Email address: ligang.feng@yzu.edu.cn; fenglg11@gmail.com (L Feng)

Experimental section

Chemicals

All chemicals were purchased and used without further purification. Ferrous sulfate heptahydrate ($FeSO_4·7H_2O$), Glycerinum ($C_3H_8O_3$ AR), Sodium hydroxide (NaOH AR), Chloroplatinic acid (H_2PtCl_6 AR), Ruthenium chloride ($RuCl_3$), sodium hypophosphite ($NaPO_2H_2$ AR), Methyl alcohol (CH_3OH AR), Ethylene glycol ($C_2H_6O_2$ AR), Nafion (AR) were purchased from Shanghai Aladdin Bio-Chem Technology Co., LTD. Commercial PtRu/C catalyst was purchased from Johnson Matthey company. Vulcan XC-72 carbon black was bought from the Cabot Co. Milli-Q water was used throughout the experiments.

Catalyst fabrication:

The α-FeOOH was synthesized by hydrothermal method firstly as follows: Glycerin (6.5 g) and $FeSO_4•7H_2O$ (0.48 g) were dissolved in 120 mL ultra-pure water and stirred magnetically for 30 minutes at room temperature. The mixed solution was put in the ultrasonic cleaning machine with ultrasonic for 20 minutes, then it was poured into 150 mL Teflon liner, packed with stainless steel kettle and put it in the oven to 110 ^oC for 12 hours. Then, centrifugal washing with ultrapure water several times after natural cooling to room temperature, and put into a vacuum drying 12 hours under 60 ^oC. The 45 mg α-FeOOH and sodium hypophosphite were placed in the same crucible. The phosphorus source was placed in the upstream of the crucible, and the α-FeOOH was placed in the downstream of the crucible. The molar ratio of Fe and P was 1:5. Then, the sample was put in the tube furnace with a heating rate at 5 ^oC / min and heated to 300 ^oC, kept 120 min in a flow of N_2 atmosphere, then naturally cooled down to room temperature. The product was obtained by centrifugation and then vacuum dried 12 h under 60 ^oC.

Take PtRu@FeP 1:1 as an example: 20.52 mg of ruthenium chloride and 100 mL of ethanediol were added into a round-bottom flask, 663 μL H_2PtCl_6 (31.5 mg mL^{-1}) was added into above solution under powerful magnetic stirring to make them fully dissolve. And then 9 mg FeP was added, keeping stirring for 30 minutes under oil bath at 150 ^{o}C for 3 hours. After that, 61 mg of carbon black was added and they were kept magnetic stirring overnight. Finally, the product was collected by suction filtration and dried 12 hours in vacuum at 60 ^{o}C. PtRu/C-H catalyst was prepared in the same way and Vulcan XC-72 carbon black was instead of FeP. PtRu@FeP 1:2 and PtRu@FeP 2:1 were prepared with the same procedure by change the molar ratio of Pt and FeP.

Characterization

The sample was characterized on Bruker D8 advance X-ray diffraction (XRD) with Cu Kα radiation. The morphology was examined with a FEI Sirion-200 scanning electron microscope (SEM) and a transmission electron microscope (TEM) operating at 200 KV. X-ray detector spectrum (EDX) images were obtained on a TECNAI G2 F30 transmission electron microscope (acceleration voltage: 300 kV). X-ray photoelectron spectroscopy (XPS) measurement was carried on an ECSALAB250Xi spectrometer with an Al Kα radiation source.

Electrochemical measurements

All the electrochemical measurements were carried out in a conventional three-electrode electrochemical cell by using an electrochemical workstation INTERFACE 1000 potentiostat/galvanostat (GAMRY INSTRUMENTS Co. USA). The saturated calomel electrode (SCE, Hg/Hg_2Cl_2) was used as the reference electrode. All of the potentials are relative to the SCE electrode. The graphite rod and the glassy carbon electrode (diameter d = 3 mm) serve as counter and working electrode, respectively. The catalyst ink was prepared as follows. 5 mg of PtRu@FeP 1:1 product, 50 μL of 5 wt %. Nafion solution was dispersed in 950 μL of ethanol by sonication for at least 30 minutes to form a homogeneous ink (loading: 20 wt% Pt and 10 wt% Ru). Then 5 μL of the catalyst ink was loaded onto a pre-cleaned working electrode and let it dry naturally.

Cyclic voltammetry was carried out at room temperature in 0.5 M H_2SO_4 containing a 1 M CH_3OH solution at the potential range between -0.2 and 1 V (vs SCE) and in 0.5 M H_2SO_4

containing a 1 M CH_3CH_2OH solution at potential range between -0.2 and 1 V (vs SCE). Chronoamperometry (CA) experiments were performed in 40 mL of 0.5 M H_2SO_4 containing 1 M CH_3OH solution at 0.6 V for 3600 s and in 40 mL of 0.5 M H_2SO_4 containing 1 M CH_3CH_2OH solution at 0.65 V for 3600 s.

The electrochemical impedance spectra (EIS) were recorded at the frequency range from 1000 kHz to 10 mHz with 15 points per decade. The amplitude of the sinusoidal potential signal was 5 mV. CO_{ads} stripping voltammetry was measured in a 0.5 M H_2SO_4 solution. CO was purged into the H_2SO_4 solution for 15 minutes to allow the complete adsorption of CO onto the catalyst when the working electrode was kept at 0 V, and excess CO in the electrolyte was purged out with N_2 for 15 min. The amount of CO_{ads} was evaluated by integration of the CO_{ads} stripping peak, assuming 420 μC cm^{-2} of coulombic charge required for the oxidation of the CO monolayer.

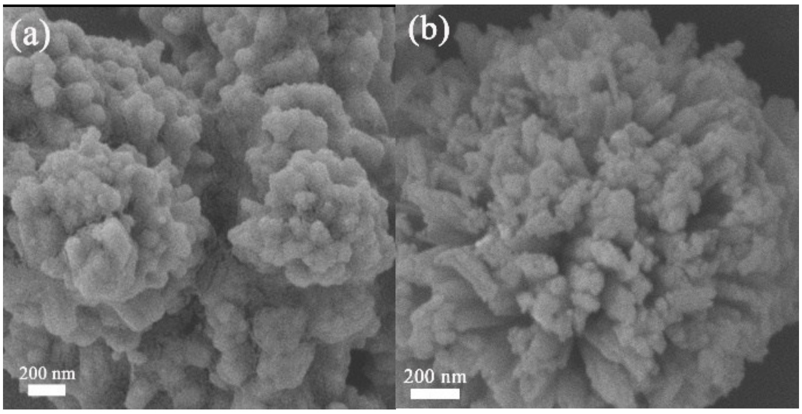

Figure S1. The SEM images of as-prepared FeP.

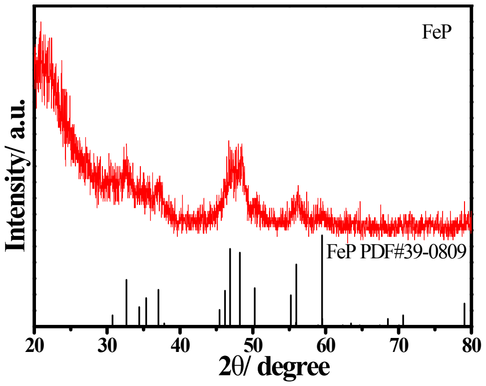

Figure S2. (a) XRD patterns of as-prepared FeP.

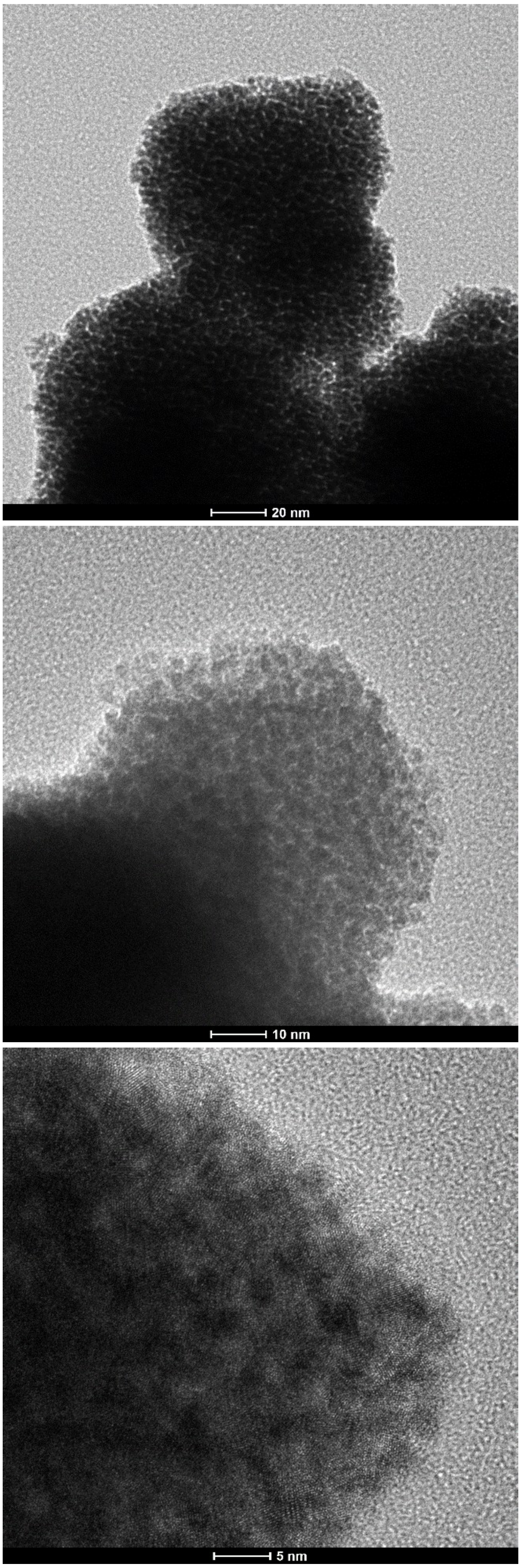

Figure S2. (b) TEM images of PtRu@FeP 1:1 catalyst.

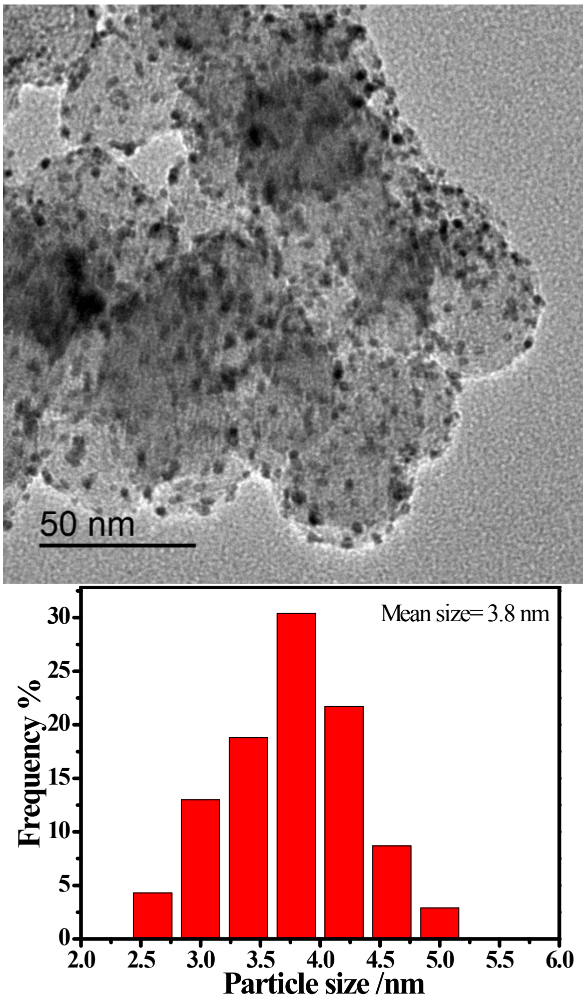

Figure S2. (c) TEM image and corresponding particle size distribution histogram of PtRu/C-JM.

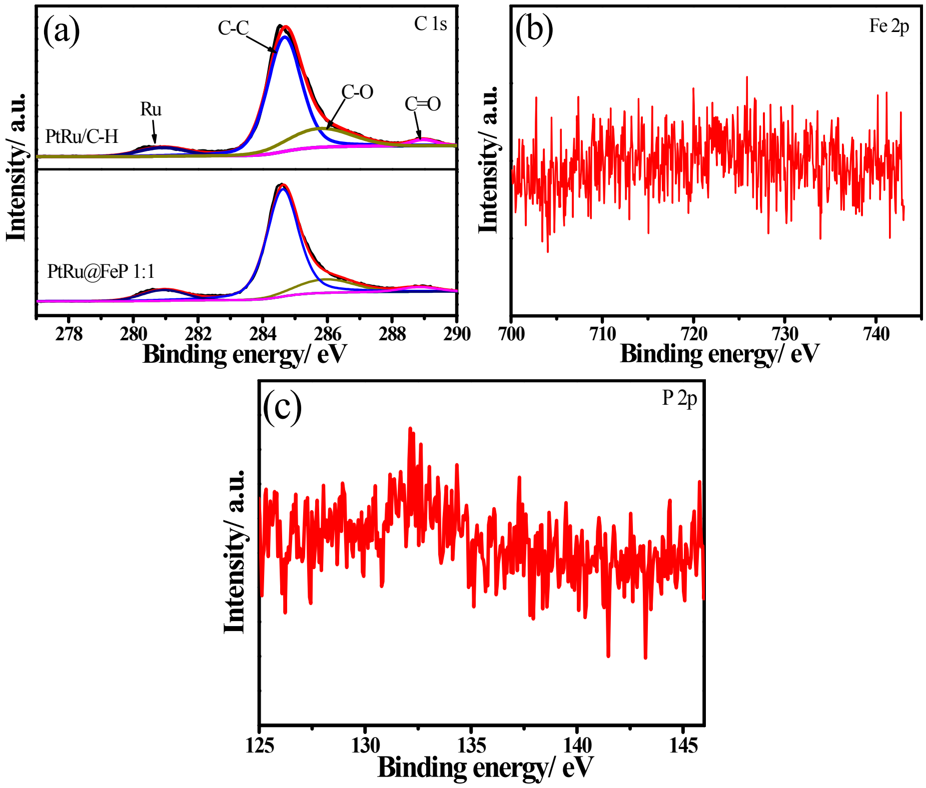

Figure S3. (a) XPS spectrum of C 1s for PtRu/C-H and PtRu@FeP 1:1catalysts. XPS spectrum of the Fe 2p (b) and P 2p (c) for PtRu@FeP 1:1 catalyst.

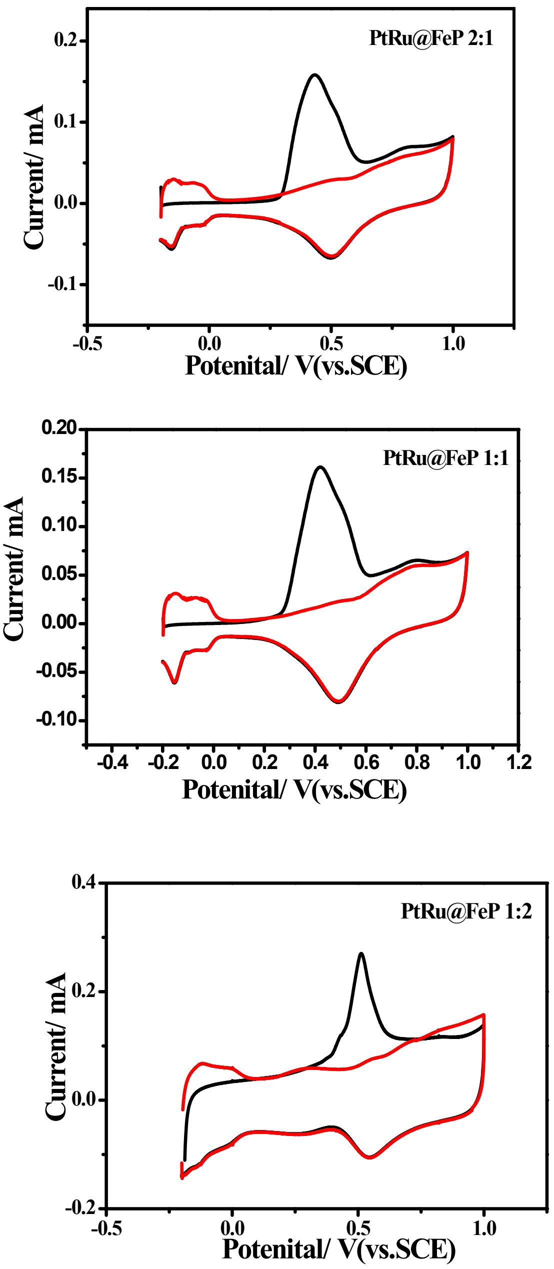

Figure S4. CO stripping voltammograms of PtRu@FeP 2:1, PtRu@FeP 1:1 and PtRu@FeP 1:2 catalysts in 0.5 M H_2SO_4 solution at a scan rate of 20 mV s^{-1}.

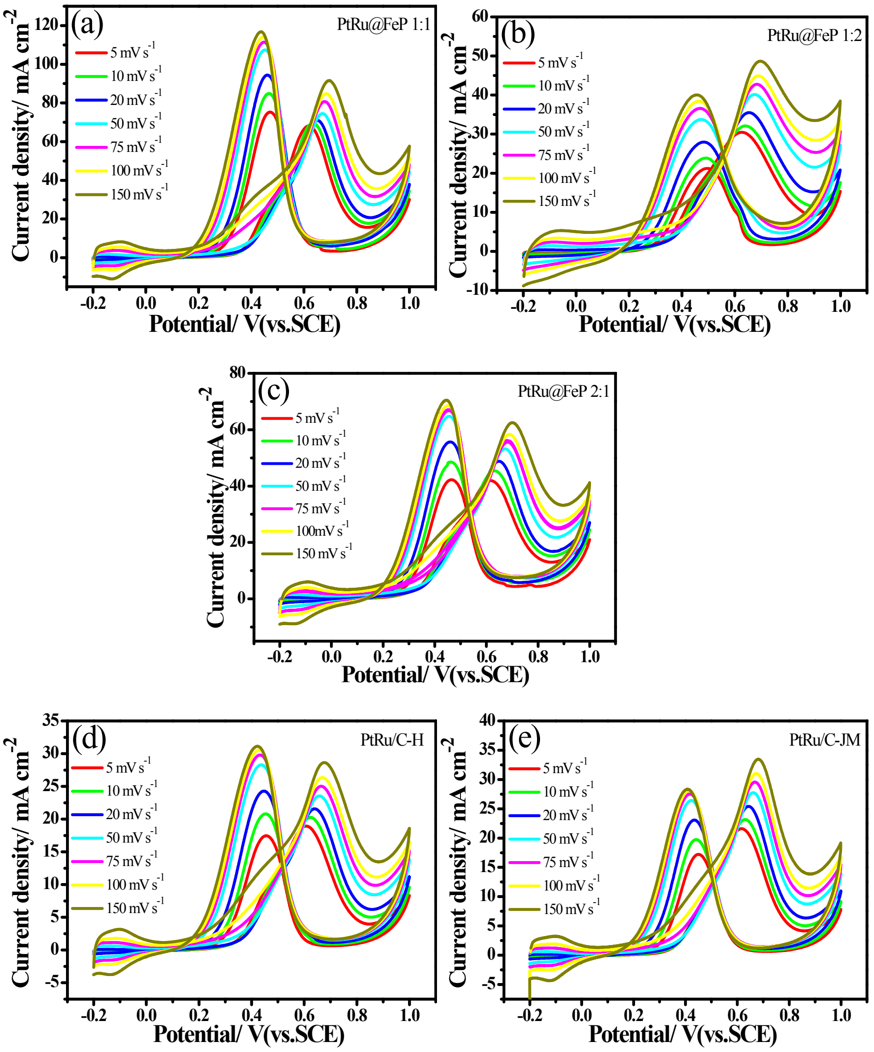

Figure S5. Cyclic voltammograms in 0.5 M H_2SO_4/1 M CH_3OH solution at scan rates of 5, 10, 20, 50, 75, 100 and 150 mV s^{-1} for PtRu@FeP 1:1 (a), PtRu@FeP 1:2 (b), PtRu@FeP 2:1 (c), PtRu/C-H (d) and PtRu/C-JM (e) catalysts.

The relationship between the peak current and the square root of scan rates complies with the following equation: $i_p=2.99\times105n(\alpha n')^{1/2}\ AC_\infty D_0{}^{1/2}\upsilon^{1/2}$. Where i_p is the peak current, n is the electron-number for the total reaction, n′ is the electron-number transferred in the rate-determining step, α is the electron transfer coefficient of the rate-determining step, A is the electrode surface area, C_∞ is the bulk concentration of the reactant, D_0 is the diffusion coefficient, υ is the potential scan rate. In this paper, the slope of the i_p vs. the square scan rate is $2.99\times105\ n(\alpha n')^{1/2}\ C_\infty D_0{}^{1/2}\upsilon^{1/2}$. In the same electrolyte and the same reaction, the parameters n, C_∞ and D_0 are constant; therefore, the slope is decided by αn′.[3]

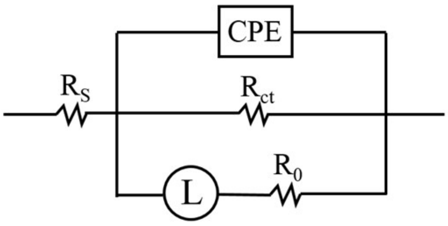

Figure S6. Equivalent circuit of Nyquist plots used for EIS data fitting.

For the equivalent circuit diagram, one of the R_S is signal of uncompensated solution resistance, R_{ct} represents the charge transfer resistance of methanol oxidation, R_0 as contact resistance between the catalyst and the electrode. The constant phase element (CPE) for double layer capacitance and the L from external circuit inductance, usually do not involve the electrochemical process.

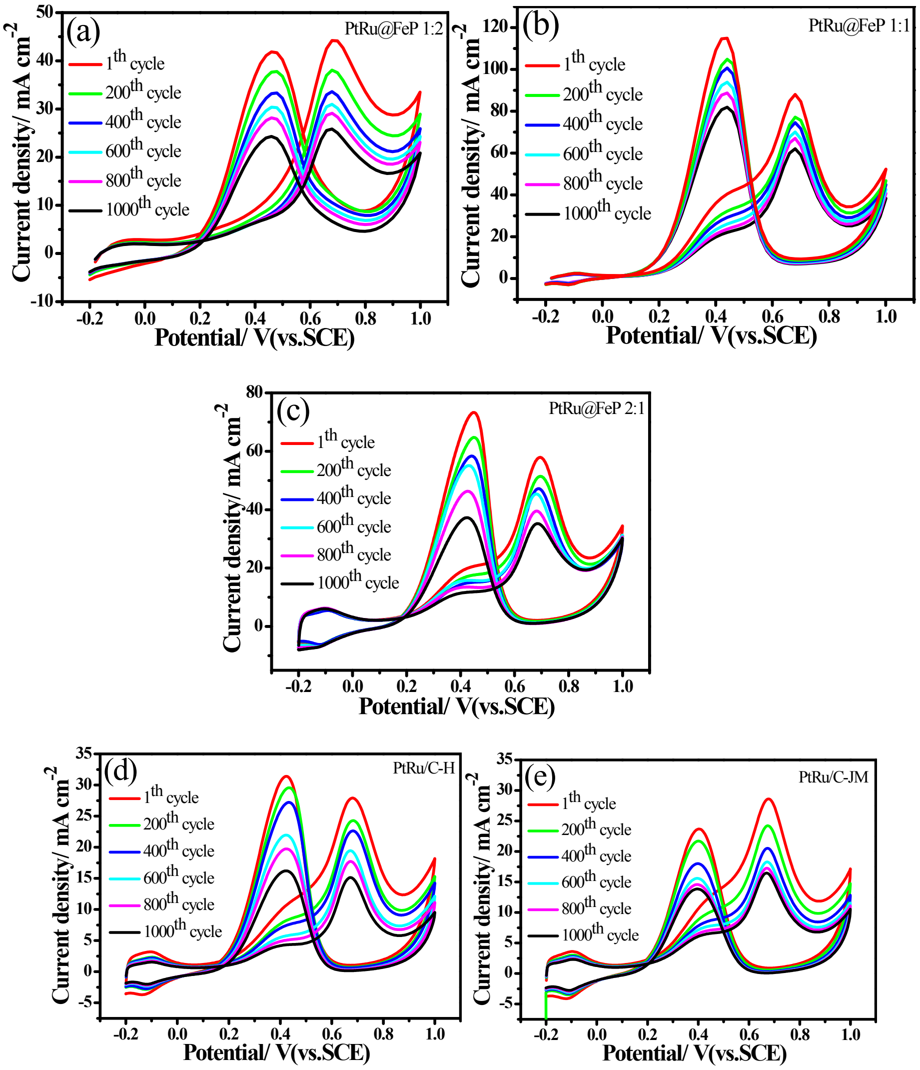

Figure S7. Cyclic voltammograms in 0.5 M H_2SO_4/1 M CH_3OH solution at 150 mV s^{-1} in an accelerated stability test for 1000 cycles for PtRu@FeP 1:1 (a), PtRu@FeP 1:2 (b), PtRu@FeP 2:1 (c), PtRu/C-H (d) and PtRu/C-JM (e) catalysts.

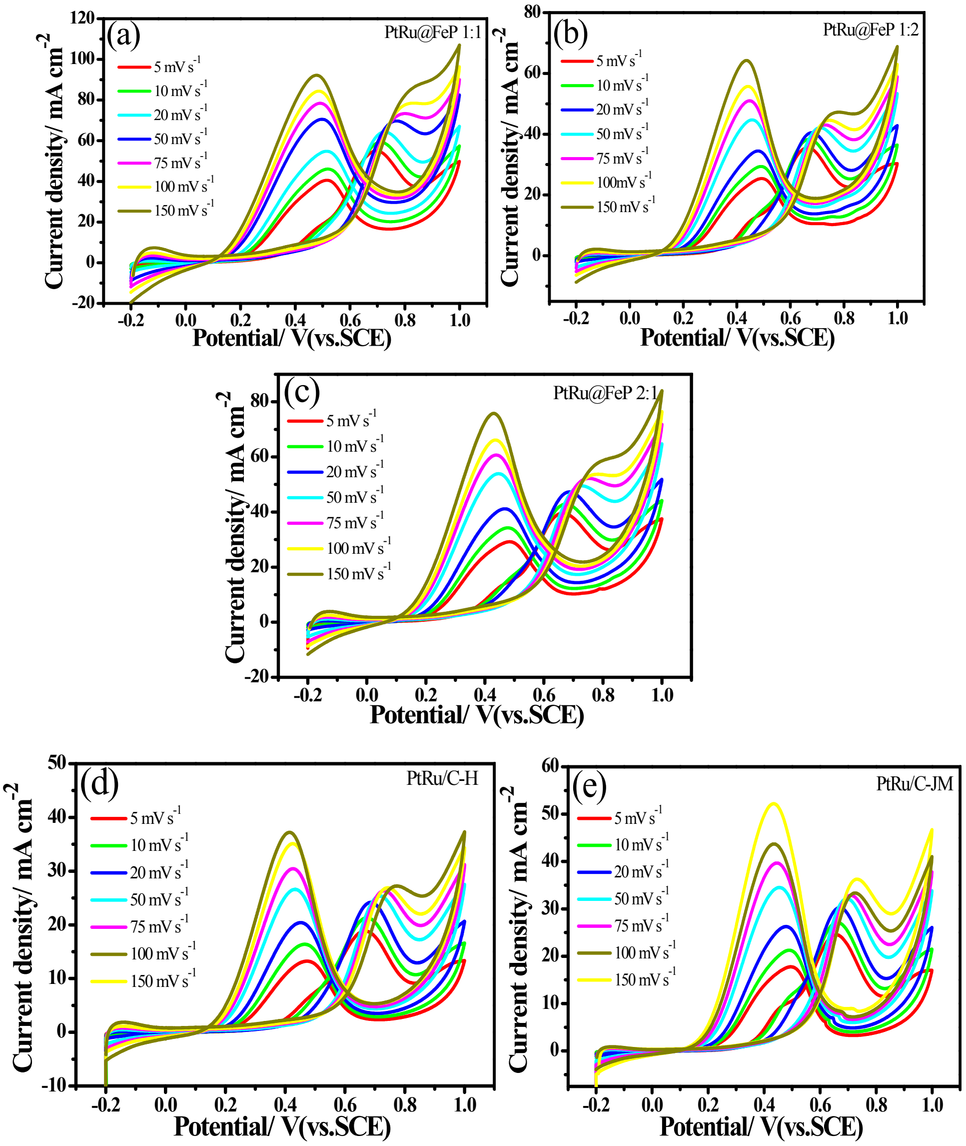

Figure S8. Cyclic voltammograms in 0.5 M H_2SO_4/1 M CH_3CH_2OH solution at scan rates of 5, 10, 20, 50, 75, 100 and 150 mV s^{-1} for PtRu@FeP 1:1 (a), PtRu@FeP 1:2 (b), PtRu@FeP 2:1 (c), PtRu/C-H (d) and PtRu/C-JM (e) catalysts.

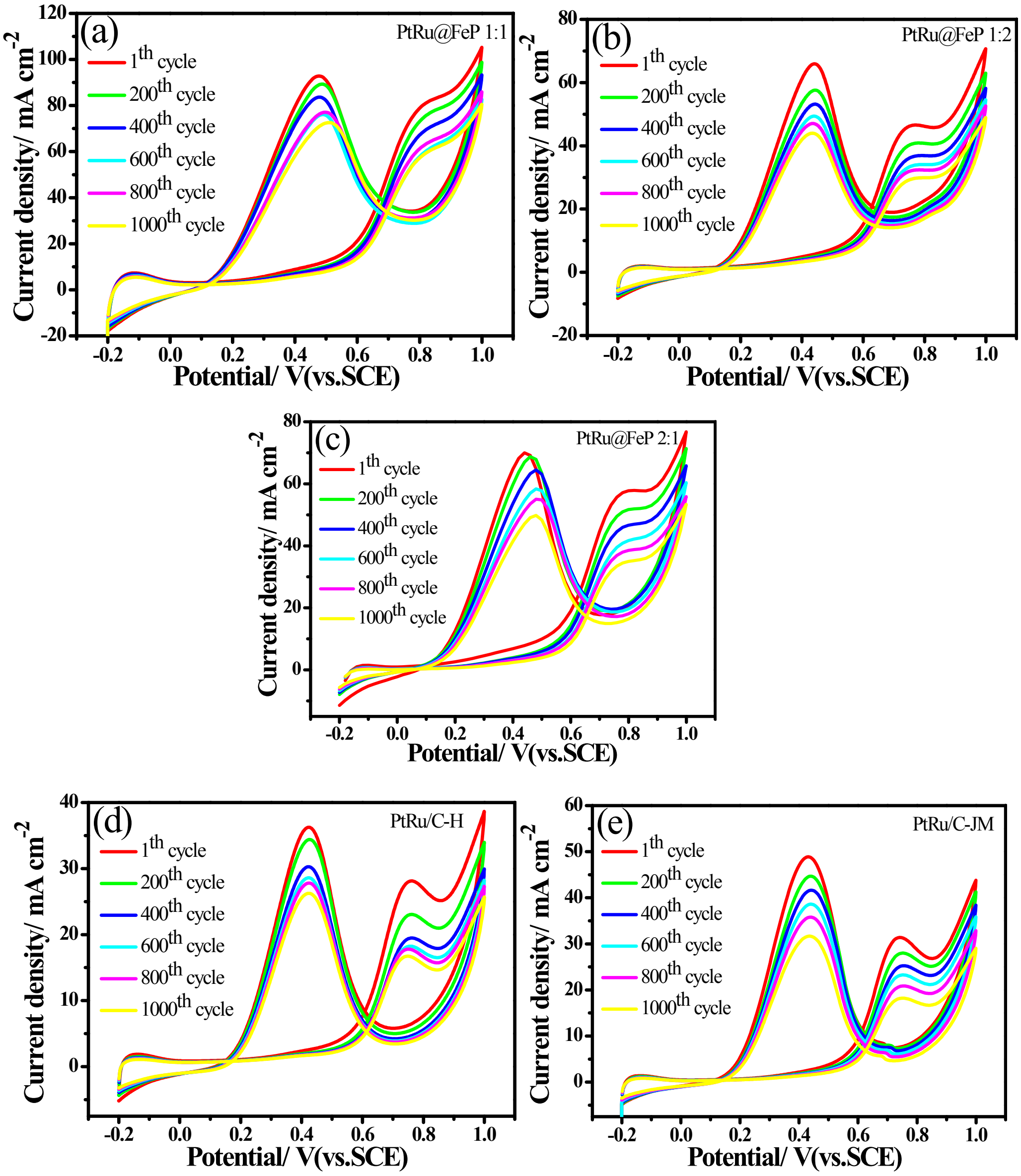

Figure S9. Cyclic voltammograms for PtRu@FeP 1:1 (a), PtRu@FeP 1:2 (b), PtRu@FeP 2:1 (c), PtRu/C-H (d) and PtRu/C-JM (e) catalysts in 0.5 M H_2SO_4/1 M CH_3CH_2OH solution at 150 mV s^{-1} in an accelerated stability test for 1000 cycles.

Table S1. Binding energy and relative intensity of Pt species obtained from curve-fitted XPS spectra for PtRu/C-JM, PtRu/C-H and PtRu@FeP 1:1 catalyst.

Catalysts	**Assignment**	**Binding energy / eV**	**Relative intensity / %**
PtRu/C-JM	Pt(0)	71.0	73.8
	Pt(II)-$Pt(OH)_2$	72.3	26.2
PtRu/C-H	Pt(0)	70.6	75.6
	Pt(II)-$Pt(OH)_2$	71.3	24.4
PtRu@FeP 1:1	Pt(0)	70.45	71.6
	Pt(II)-$Pt(OH)_2$	71.45	28.4

Table S2. Binding energy and relative intensity of Ru species obtained from curve-fitted XPS spectra for PtRu/C-JM, PtRu/C-H and PtRu@FeP 1:1 catalyst.

Catalysts	**Assignment**	**Binding energy / eV**	**Relative intensity / %**
PtRu/C-JM	Ru(0)	461.3	53.2
	Ru(IV)-RuO_2	462.8	31.7
	Hydrous Ru oxides (RuO_xH_y)	465.1	15.1
PtRu/C-H	Ru(0)	461.2	50.1
	Ru(IV)-RuO_2	463.0	38.8
	Hydrous Ru oxides (RuO_xH_y)	465.9	11.1
PtRu@FeP 1:1	Ru(0)	460.8	55.1
	Ru(IV)-RuO_2	462.4	31.2
	Hydrous Ru oxides (RuO_xH_y)	464.6	13.7

Table S3. Electrochemical surface area (ECSA) estimated from CO stripping experiments, the peak potential and the onset potential for CO oxidation for the relevant catalysts.

Catalysts	ECSA /m^2 g^{-1}	Peak Potential /V vs. SCE	Onset Potential /V vs. SCE
PtRu@FeP 1:2	61	0.51	0.31
PtRu@FeP 1:1	71	0.42	0.25
PtRu@FeP 2:1	66	0.43	0.30
PtRu/C-H	44	0.53	0.32
PtRu/C-JM	50	0.53	0.31

Table S4. Peak current density, onset potential, mass activity and specific activity for different catalyst samples for methanol oxidation.

Catalysts	Peak Current Density /mA cm^{-2}	Onset Potential /V vs. SCE	Mass Activity /mA mg$^{-1}_{PtRu}$	Specific Activity /mA cm^{-2}
PtRu@FeP 1:2	40	0.34	373	0.61
PtRu@FeP 1:1	75	0.28	700	1
PtRu@FeP 2:1	54	0.28	504	0.76
PtRu/C-H	23	0.38	215	0.49
PtRu/C-JM	28	0.38	267	0.53

Table S5. The comparison of different catalyst in acid electrolyte for methanol oxidation.

Catalysts	Onset Potential /V vs. SCE	Mass Activity /mA mg^{-1}_{PtRu}	Specific Activity /mA cm^{-2}	electrolyte	reference
PtRu@FeP 1:1	0.28	700	1	0.5 M H_2SO_4 + 1 M CH_3OH.	This work
PtFe@PtRuFe	0.416	690	1.3	0.1 M $HClO_4$+ 0.5 M CH_3OH	4
NPG-Pt_2Ru_1	/	/	0.44	0.5 M H_2SO_4 + 0.5 M CH_3OH.	5
Pt-Ag HI	0.4	400	/	1 M H_2SO_4 + 1 M CH_3OH.	6
PtRu/ND + AB (4:1)	/	130	/	0.5 M H_2SO_4 + 1.0 M CH_3OH	7
Pt_1Ru_2/C	/	681 mA mg^{-1}_{Pt}	/	0.1 M $HClO_4$ + 0.5 M CH_3OH.	8
PtRu/RGO/TNTs	/	0.316	/	0.5 M H_2SO_4 + 1.0 M CH_3OH	9
PtRu/90C.10Mn_3O_4	/	437.4	/	0.5 M H_2SO_4 + 1.0 M CH_3OH	10
Pt_7Ru_2Fe	0.44	/	1.1	0.1 M $HClO_4$ + 0.5 M CH_3OH.	11
Ru@$Pt_{0.5}$/C	/	1313.8 mA mg^{-1}_{Pt}	/	0.5 M H_2SO_4 + 1.0 M CH_3OH	12
PdCu@Pt/C	/	2270 mA mg^{-1}_{Pt}	/	0.5 M H_2SO_4 + 1.0 M CH_3OH	13
H–PtRu	0.44	/	0.62	0.5 M H_2SO_4 + 1.0 M CH_3OH	14
PtRu@TiO_2	/	/	0.478	0.5 M H_2SO_4 + 0.5 M CH_3OH	15

Table S6. EIS fitting parameters from equivalent circuit for different catalyst for methanol oxidation.

Catalysts	R_S / Ω cm^2	CPE-Yo /S s^{-n} cm^2	CPE-n	R_{CT} / Ω cm^2	L / H cm^2	R_0 / Ω cm^2	Chi squared
PtRu@FeP 1:2	7.5	1.1 E-3	0.8	754	2.1 E+3	44	1.4 E-2
PtRu@FeP 1:1	8.2	1.8 E-3	0.8	450	7.4 E+2	60	1.2 E-2
PtRu@FeP 2:1	7.6	1.5 E-3	0.8	650	1.1 E+3	168	5.7 E-2
PtRu/C-H	9.9	4.7 E-4	0.9	1632	9.4 E+3	36	1.0 E-1
PtRu/C-JM	10	3.4 E-4	0.9	1550	5.1 E+3	1.3 E-2	8.6 E-2

Table S7. Peak current density, onset potential, mass activity and specific activity of different catalyst for ethanol oxidation.

Catalysts	Peak Current Density /mA cm^{-2}	Onset Potential /V vs. SCE	Mass Activity /mA mg$^{-1}_{PtRu}$	Specific Activity /mA cm^{-2}
PtRu@FeP 1:2	42	0.38	392	0.64
PtRu@FeP 1:1	70	0.34	653	0.92
PtRu@FeP 2:1	50	0.38	467	0.71
PtRu/C-H	25	0.52	233	0.53
PtRu/C-JM	32	0.47	298	0.60

Table S8. The comparison of onset potential, mass activity and specific activity for different catalyst samples in acid electrolyte for ethanol oxidation.

Catalysts	Onset Potential /V vs. SCE	Mass Activity /mA mg^{-1}_{PtRu}	Specific Activity /mA cm^{-2}	electrolyte	reference
PtRu@FeP 1:1	0.34	653	0.92	0.5 M H_2SO_4 + 1 M CH_3CH_2OH	This work
PtRuNi/C	0.55	/	/	0.5 M H_2SO_4 + 0.5 M CH_3CH_2OH	16
PtRu/C-Sb	/	190	/	0.1 M $HClO_4$ + 1 M CH_3CH_2OH	17
PtRu/C	0.28	357	/	0.5 M H_2SO_4 + 0.5 M CH_3CH_2OH	18
PtRuCu/NTA	/	630	/	1 M H_2SO_4 + 0.5 M CH_3CH_2OH	19
Pt-Ru/C BX0	0.26	434	/	0.5 M H_2SO_4 + 0.5 M CH_3CH_2OH	20
Pt_1Ru_1/C	/	811 mA mg^{-1}_{Pt}	/	0.5 M H_2SO_4 + 0.5 M CH_3CH_2OH	8
Ru@PtPd/C	/	3600 mA mg^{-1}_{PtPd}	/	1 M KOH + 1 M CH_3CH_2OH	21
Ru@Pt	0.37	/	/	0.5 M H_2SO_4 + 0.5 M CH_3CH_2OH	22
Ni@PbPt/G	0.29	281 mA mg^{-1}_{Pt}	/	0.5 M H_2SO_4 + 1 M CH_3CH_2OH	23

Table S9. EIS fitting parameters from equivalent circuits for different catalyst samples for ethanol oxidation.

Catalysts	R_S / Ω cm^2	CPE-Yo /S s^{-n} cm^2	CPE-n	R_{CT} / Ω cm^2	L / H cm^2	R_0 / Ω cm^2	Chi squared
PtRu@FeP 1:2	9.2	5.2 E-4	0.8	1598	2.3 E+3	427	2 E-2
PtRu@FeP 1:1	9	1.3 E-3	0.8	893	7.3 E+3	2.4 E-4	5.7 E-3
PtRu@FeP 2:1	8.9	6.1 E-4	0.8	1150	3.9 E+3	5.4	9.3 E-2
PtRu/C-H	8.8	4.9 E-4	0.8	1695	8.3 E+3	78	6.3 E-2
PtRu/C-JM	7.4	3.1 E-4	0.8	1550	3.4 E+3	259	8.4 E-3

Reference

1 T. Iwasita, *Electrochim. Acta*, 2002, **47**, 3663-3674.

2 F. Colmati, E. Antolini and E. R. Gonzalez, *Journal of Power Sources*, 2006, **157**, 98-103.

3 L. Feng, X. Zhao, J. Yang, W. Xing and C. Liu, *Catal. Commun.*, 2011, **14**, 10-14.

4 Q. Wang, S. Chen, P. Li, S. Ibraheem, J. Li, J. Deng and Z. Wei, *Applied Catalysis B: Environmental*, 2019, **252**, 120-127.

5 M. Tian, S. Shi, Y. Shen and H. Yin, *Electrochim. Acta*, 2019, **293**, 390-398.

6 T. Radhakrishnan and N. Sandhyarani, *Electrochimica Acta*, 2019, **298**, 835-843.

7 Y. Zhang, Y. Wang, L. Bian, R. Lu and J. Zang, *Applied Surface Science*, 2016, **364**, 645-650.

8 Y. Hu, A. Zhu, Q. Zhang and Q. Liu, *Int. J. Hydrogen Energy*, 2016, **41**, 11359-11368.

9 J. Han, L. Yang, L. Yang, W. Jiang, X. Luo and S. Luo, *Int. J. Hydrogen Energy*, 2018, **43**, 7338-7346.

10 V. Comignani, J. M. Sieben, M. E. Brigante and M. M. E. Duarte, *ChemElectroChem*, 2018, **5**, 2118-2125.

11 M. E. Scofield, C. Koenigsmann, L. Wang, H. Liu and S. S. Wong, *Energy & Environmental Science*, 2015, **8**, 350-363.

12 J. Xie, Q. Zhang, L. Gu, S. Xu, P. Wang, J. Liu, Y. Ding, Y. F. Yao, C. Nan, M. Zhao, Y. You and Z. Zou, *Nano Energy*, 2016, **21**, 247-257.

13 H. Wang, R. Wang, H. Li, Q. Wang, J. Kang and Z. Lei, *Int. J. Hydrogen Energy*, 2011, **36**, 839-848.

14 Y. Hu, A. Zhu, Q. Zhang and Q. Liu, *Journal of Power Sources*, 2015, **299**, 443-450.

15 Y. Hu, A. Zhu, C. Zhang, Q. Zhang and Q. Liu, *Int. J. Hydrogen Energy*, 2015, **40**, 15652-15662.

16 P.-J. Z. Zhen-Bo Wang, Guang-Jin Wang, Chun-Yu Du, and Ge-Ping Yin, *J. Phys. Chem. C*, 2008.

17 M. C. Figueiredo, O. Sorsa, R. M. Arán-Ais, N. Doan, J. M. Feliu and T. Kallio, *J. Catal.*, 2015, **329**, 69-77.

18 S. Themsirimongkon, T. Sarakonsri, S. Lapanantnoppakhun, J. Jakmunee and S. Saipanya, *Int. J. Hydrogen Energy*, 2018.

19 V. Comignani, J. M. Sieben, M. D. Sanchez and M. M. E. Duarte, *Int. J. Hydrogen Energy*, 2017, **42**, 24785-24796.

20 D. González-Quijano, W. J. Pech-Rodríguez, J. A. González-Quijano, J. I. Escalante-García, G. Vargas-Gutiérrez, I. Alonso-Lemus and F. J. Rodríguez-Varela, *Int. J. Hydrogen Energy*, 2015, **40**, 17291-17299.

21 H. Gao, S. Liao, Z. Liang, H. Liang and F. Luo, *Journal of Power Sources*, 2011, **196**, 6138-6143.

22 N. M. Sánchez-Padilla, S. M. Montemayor, L. A. Torres and F. J. Rodríguez Varela, *Int. J. Hydrogen Energy*, 2013, **38**, 12681-12688.

23 D. Chen, Y. Zhao, Y. Fan, X. Peng, X. Wang and J. Tian, *J. Mater. Chem. A*, 2013, **1**, 13227-13232.